Nanobacteria: An alternative mechanism for pathogenic intra- and extracellular calcification and stone formation

E. OLAVI KAJANDER* AND NEVA ÇIFTÇIOGLU

Department of Biochemistry and Biotechnology, University of Kuopio, P.O.B. 1627, Fin-70211, Kuopio, Finland

ABSTRACT Calcium phosphate is deposited in many diseases, but formation mechanisms remain speculative. Nanobacteria are the smallest cell-walled bacteria, only recently discovered in human and cow blood and commercial cell culture serum. In this study, we identified with energy-dispersive x-ray microanalysis and chemical analysis that all growth phases of nanobacteria produce biogenic apatite on their cell envelope. Fourier transform IR spectroscopy revealed the mineral as carbonate apatite. The biomineralization in cell culture media resulted in biofilms and mineral aggregates closely resembling those found in tissue calcification and kidney stones. In nanobacteria-infected fibroblasts, electron microscopy revealed intra- and extracellular acicular crystal deposits, stainable with von Kossa staining and resembling calcospherules found in pathological calcification. Previous models for stone formation have led to an hypothesis that elevated pH due to urease and/or alkaline phosphatase activity is a lithogenic factor. Our results indicate that carbonate apatite can be formed without these factors at pH 7.4, at physiological phosphate and calcium concentrations. Nanobacteria can produce apatite in media mimicking tissue fluids and glomerular filtrate and provide a unique model for *in vitro* studies on calcification.

The formation of discrete and organized inorganic crystalline structures within macromolecular extracellular matrices is a widespread biological phenomenon generally referred to as biomineralization. Mammalian bone and dental enamel are examples of biomineralization involving apatite minerals. The molecular basis of mineralization remains largely unknown (1). Recently, bacteria have been implicated as factors in biogeochemical cycles for mineral formation in aqueous sediments (2, 3). The principal constituent of modern authigenic phosphate minerals in marine sediments is carbonate (hydroxy)fluorapatite $Ca_{10}(PO_4)_{6-x}(CO_3)_x(F,OH)_{2+x}$. Microorganisms are capable of depositing apatite outside thermodynamic equilibrium in sea water. They can segregate Ca from Mg and actively nucleate carbonate apatite by means of specific oligopeptides under conditions pH < 8.5 and [Mg]:[Ca] > 0.1 (4). Such conditions are also present in the human body.

We have discovered nanobacteria in human and cow blood that are cytotoxic *in vitro* (5) and *in vivo* (6). They have been deposited in DSM (no. 5819–5821; Braunschweig, Germany). Nanobacteria possess unusual properties, making their detection difficult with standard microbiological methods. Although they typically had diameters of 0.2–0.5 μm, they passed through 0.1-μm filters probably because tiny forms (0.05–0.2 μm) were also observed in transmission electron microscopy (TEM) (7). Nanobacteria were poorly disruptable, stainable, fixable, and exceptionally resistant to heat (8, 9). Their doubling time was about 3 days. High doses of γ-irradiation or aminoglycoside antibiotics prevented their multiplication. According to the 16S rRNA gene sequence (EMBL X98418 and X98419), nanobacteria fall within the α-2 subgroup of Proteobacteria, which also includes *Brucella* and *Bartonella* species (10). The latter genera include human and animal pathogens that share similarities with nanobacteria, e.g., some antigens (our unpublished data), intra- and extracellular location in the host, and cytopathic effects (5).

In this study, we provide evidence that nanobacteria can act as crystallization centers (nidi) for the formation of biogenic apatite structures. The mineralization process was studied *in vitro* with one bovine isolate from commercial fetal bovine serum (FBS) and with a human isolate. Our findings are of concern in medicine because nanobacterial bacteremia occurs in humans, and nanobacterial nidi might initiate pathological calcification.

MATERIALS AND METHODS

Culture Methods for Nanobacteria. Nanobacteria were cultured in DMEM (GIBCO) under mammalian cell culture conditions (37°C; 5–10% CO_2/90–95% air). Serum was used at a 10% final concentration as the supplement and source of nanobacteria, which were FBS (lot 901045; Sera-Lab, Crawley Down, Sussex, U.K.) or human serum from a 29-years-old Finnish male, as described previously (5). The cultures were prepared using strict aseptic techniques in a cell culture facility. Nanobacterial samples were filtered through 0.2-μm filters before culturing. Subcultures were made using either the same serum or γ-irradiated FBS (γ-FBS) as a culture supplement. FBS and nanobacteria were γ-irradiated, when indicated, at a minimum dose of 30 kGy given at room temperature during about 16 hr (Kolmi-Set, Ilomantsi, Finland).

Subculturing of nanobacteria in serum-free (SF) DMEM was performed with monthly passages 1:11 for 5 yr. SF nanobacteria attach firmly to the bottom of the culture vessel. These cultures were passaged or harvested with a rubber scraper. Cultures were established on Loeffler medium supplemented with 10% conditioned medium from nanobacterial culture, and DMEM replaced water in the formula (11). The incubation period was 6 wk under cell culture conditions.

Only pure nanobacterial cultures were used. Positive identification of nanobacteria involved typical growth rates and optical properties, specific stainability with Hoechst 33258 and with indirect immunofluorescence staining (IIFS), as described below. Control experiments were performed to determine whether spontaneous crystallization could occur in a culture medium. The medium was incubated with or without

---

Abbreviations: AP, alkaline phosphatase; DIC, differential interference contrast; EDX, energy-dispersive x-ray microanalysis; FBS, fetal bovine serum; γ-FBS, γ-irradiated FBS; FTIR, Fourier transform IR spectroscopy; IIFS, indirect immunofluorescence staining; SEM, scanning electron microscopy; SF, serum free; SF nanobacteria, nanobacteria cultured under serum-free conditions; TEM, transmission electron microscopy.
A commentary on this article begins on page 7846.
*To whom reprint requests should be addressed. e-mail: Olavi. Kajander@uku.fi.

Medical Sciences: Kajander and Çiftçioglu

Proc. Natl. Acad. Sci. USA 95 (1998)   8275

γ-FBS or γ-irradiated nanobacteria (10). Neither mineralization nor nanobacteria multiplication was observed even during the 6-mo follow-up.

Preparation and Infection of 3T6 Cells. 3T6 cells (ATCC CCL 96) were cultured on coverslips as described before (5). SF nanobacterial cultures were scraped and 100-μl portions were added to the cell cultures and incubated for 24 hr in the

incubator. Only DMEM was added to the control experiments. TEM, IIFS (5), and DNA and von Kossa staining were used for the observation of the cell–SF nanobacteria interaction.

Kidney Stones. Thirty randomly collected kidney stones (K-SKS; Stone Analysis Central Laboratory, Jyväskylä, Finland) were demineralized in 1 M HCl and then neutralized (2), centrifuged at 14,000 × g for 15 min, and the pellets used for
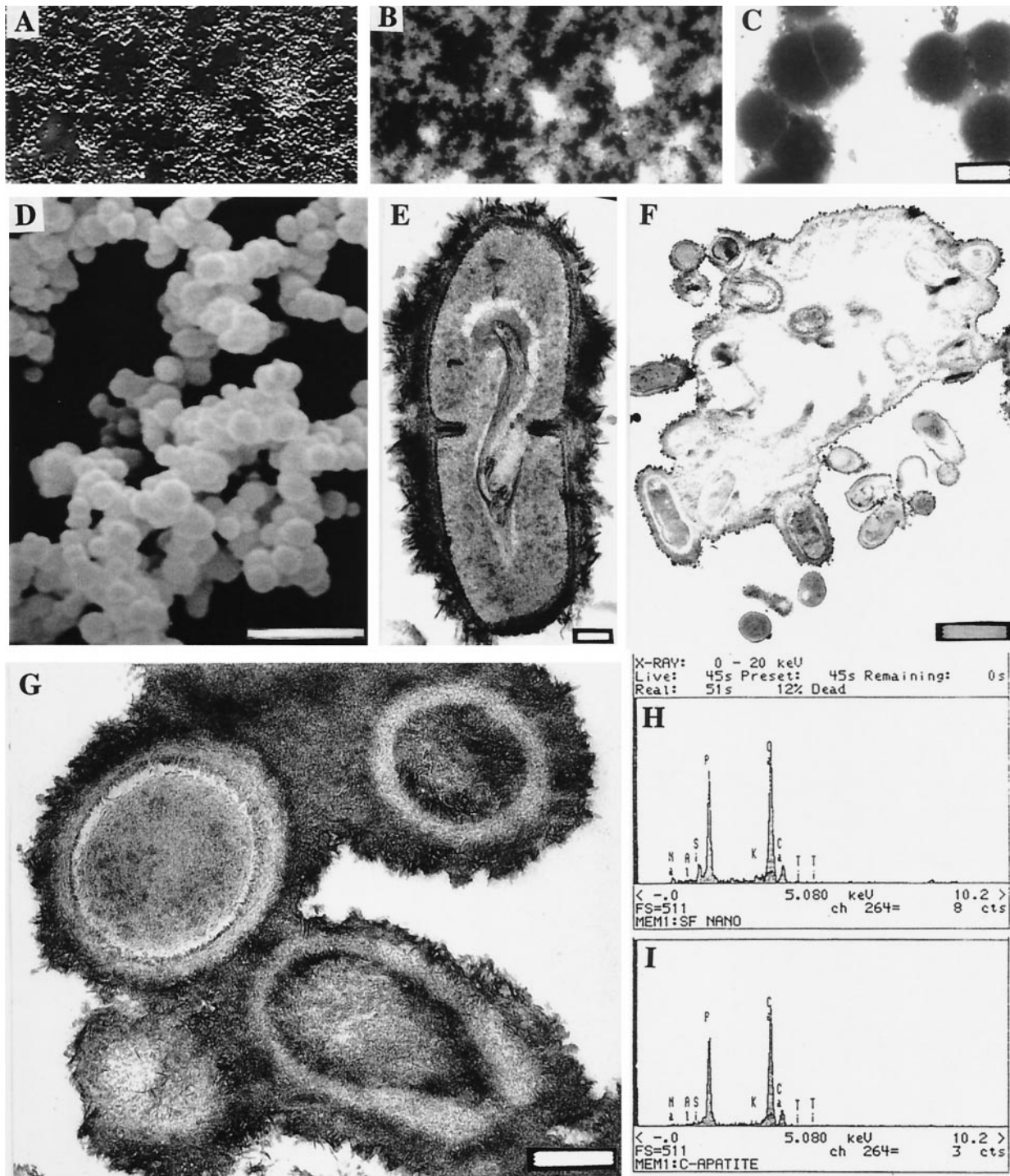

FIG. 1. Light and electron microscopic images of nanobacteria and their analyses with EDX. (*A*) DIC image of bottom-attached nanobacteria after a 2-mo culture period. (*B*) DNA staining of the same area (×1600) with the modified Hoechst method. (*C*) Negative staining of nanobacteria isolated directly from FBS. (Bar = 200 nm.) (*D*) SEM micrograph showing their variable size. (Bar = 1 μm.) (*E*) A dividing nanobacterium covered with a "hairy" apatite layer. (Bar = 100 nm.) (*F*) TEM micrograph of nanobacteria buried in an apatite layer after a 3-mo culture period (bar = 1 μm) and *G* at higher magnification (bar = 200 nm). White central areas in *F* are artifacts due to loss of the mineral layer in sectioning. (*H*) EDX analysis in SEM of nanobacteria showing Ca and P peaks similar to those of hydroxyapatite (*I*).

IIFS and TEM. Part of the pellets were suspended in DMEM, sterile-filtered, and cultured in DMEM supplemented with γ-FBS under nanobacterial culture conditions.

Staining Methods. DNA stainings with Hoechst 33258 fluorochrome were carried out as described in a Hoechst Stain kit (Flow Laboratories), except where indicated, increasing the stain concentration from 0.5 μg/ml to 5 μg/ml (7). IgG$_1$ class anti-nanobacterial mAbs, Nb 8/0 and Nb 5/2, were used in IIFS (5). The epitope of the latter mAb was inactivated by incubating it in sodium borohydrate (3 × 1 min; 0.5 mg/ml in PBS), when indicated, to test specificity of the binding. The samples were viewed under a Nikon Microphot-FXA microscope with fluorescence and differential interference contrast (DIC) optics. Specific calcification detection was performed with von Kossa staining (12). 3T6 cells exposed to SF nanobacteria for 48 hr were used as samples.

Electron Microscopy and Energy Dispersive X-Ray Microanalysis (EDX). For negative staining, nanobacteria were isolated by centrifugation at 40,000 × g for 1 hr directly from FBS diluted 1:5 in PBS. A carbon-coated 400 mesh copper grid was placed on a drop of the suspension of nanobacteria in PBS for 1 min, washed with water, and stained on a drop of 1% phosphotungstic acid for 90 sec. Scanning electron microscopy (SEM) and TEM were performed as described previously (5). The topographic features of the nanobacteria were investigated with a scanning electron microscope equipped with EDX as described previously (13). Hydroxyapatite (No-H-0252; Sigma) was used as a reference.

Fourier Transform IR Spectroscopy (FTIR), Chemical Analysis, and Enzyme Assays. Hydroxyl and carbonate groups in the apatite minerals were detected by FTIR in the K-SKS (Stone Analysis Central Laboratory) following the standard method (14). Chemical analysis of nanobacteria was carried out as described previously (15). Urease enzyme activity was analyzed using the standard method (16) and alkaline phosphatase (AP) with *p*-nitrophenylphosphate as substrate at pH 9.5.

RESULTS

Culture Properties, Morphology, and Apatite Formation by Nanobacteria in Serum-Containing Media. Light microscopy with DIC optics revealed barely detectable nanobacteria near the bottom of the culture vessel after about a 1-wk culture period. In 2 wk, nanobacteria appeared as groups easily visible in microscopy. After 1 mo, many were in clumps and started to attach to the bottom of the culture vessel, and by the end of 2 mo, most were in a white-colored biofilm visible to the naked eye. The criteria for pure nanobacterial culture were refractile aggregates of typical coccoid-shaped particles (Fig. 1*A*), showing DNA stainability (Fig. 1*B*) only with the modified method, a negative culture result on sheep blood agar, and IIFS positivity with anti-nanobacteria mAbs (5).

Negative-staining of nanobacteria in uncultured FBS revealed 0.2- to 0.3-μm coccoid particles (Fig. 1*C*). After a 1-mo culture period, SEM revealed similar coccoid shapes with a diameter of 0.2–0.5 μm (Fig. 1*D*). Their rough surfaces resembled those seen in TEM (Fig. 1 *E–G*). During longer culture periods, they were mostly attached to the culture vessel and finally were in a mineral layer (Fig. 1 *F* and *G*). Chemical analysis using EDX gave similar Ca and P peaks as detected for hydroxyapatite (Fig. 1 *H* and *I*). Cultures of the human isolate gave identical results (not shown). Chemical analysis of nanobacteria harvested after a 3-mo culture period revealed a high content of inorganic material. The pellet dry weight varied from 23 to 39% and consisted of: N, 1–1.3%; P, 12.3–14.6%; Ca, 23.4–23.5%; Mg, 1.4–1.9%; K, 0.1%; and Na, 1.2–1.4%. FTIR revealed that carbonate apatite was present in samples from all culture ages between 7 and 180 days in both human and bovine nanobacteria. Control hydroxyapatite was correctly identified in the test. The analytical methods do not
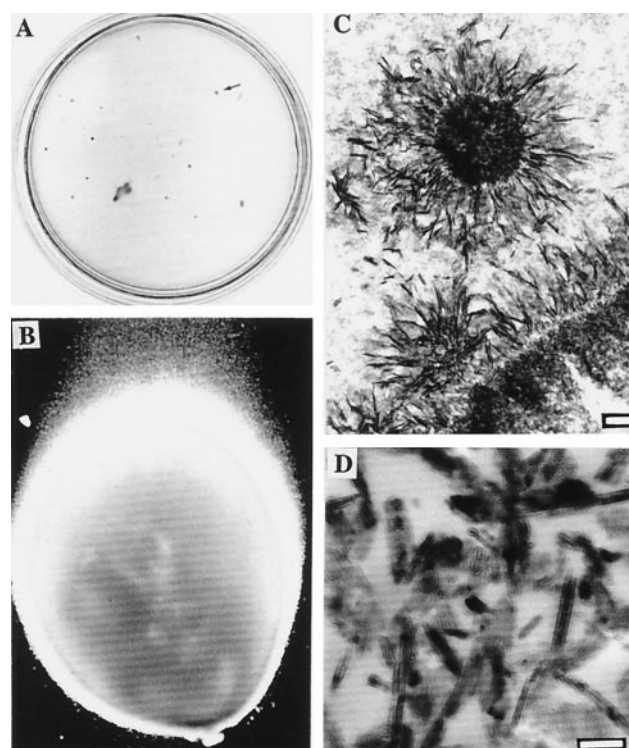

Fig. 2.   Nanobacterial stony colonies and comparison to hydroxyapatite. (*A*) Colonies on modified Loeffler medium in a 10-cm plate. The colonies penetrated through the medium forming stony pillars. Arrow shows one typical grayish brown colony depicted in *B*. (×40.) (*C*) Needle-like crystal deposits in the pillar revealed by TEM. (Bar = 200 nm.) (*D*) TEM image of reference apatite crystals. (Bar = 100 nm.)

exclude the possible presence of minor quantities of other mineral phases. To exclude that possibility, crystallographic analysis is needed. Nanobacteria did not produce urease or AP activity, and their culture medium remained at pH 7.4.

Apatite Formation by Nanobacteria in Loeffler Medium. Macroscopic nanobacterial colonies on modified Loeffler medium (Fig. 2 *A* and *B*) were stony, grayish brown, passagable, and penetrated the medium layer and attached to the bottom of the culture vessel after 6 wk of culture. IIFS with anti-nanobacteria mAbs (data not shown) and TEM revealed nanobacteria coated in needle-like apatite crystals (Fig. 2*C*) similar to the hydroxyapatite crystals (Fig. 2*D*).

Apatite Formation by Nanobacteria in SF Medium. When washed nanobacterial pellets or SF nanobacteria were subcultured in SF DMEM, bottom-attached coccoid organisms were observed within 1 day. DIC microscopy revealed a several-micrometer-thick mineral layer around each nanobacteria, reaching a yeast size within 1 wk (Fig. 3*A*). Their morphology differed extensively from the coccoid nanobacteria, but similar DNA stainability was observed (Fig. 3*B*). They produced biomass at about half the rate observed in serum-containing cultures. The metabolic incorporation of [^{35}S]methionine and [5-^{3}H]uridine is proof that they were replicating (17). DIC microscopy revealed nanobacterial multiplication inside the mineral formations (Fig. 3*C*). These apatite shelters, were shown in SEM to have a hollow interiors, were apparently the dwelling place of the organisms (Fig. 3 *E* and *F*). The size of the cavity is probably dependent on the number of nanobacteria it contains (Fig. 3*F*). Apparently, the openings of the cavities were facing the bottom of the culture vessel before scraping. Thus, the apatite shelters provided complete protection for the organisms. The cultures could be passaged monthly for over 5 yr and always followed a similar growth pattern. After addition of γ-FBS, these nanobacterial formations re-

Medical Sciences: Kajander and Çiftçioglu

Proc. Natl. Acad. Sci. USA 95 (1998)   8277

turned to the forms found in serum cultures (see Fig. 3D). That the shelters were apatite in nature was proven by EDX. FTIR determined that it was carbonate apatite. The human isolate produced similar formations.

Intra- and Extracellular Calcification in Fibroblast Cultures. 3T6 cells infected for 48 hr with SF nanobacteria showed altered cell morphology, e.g., large vacuolization with internalized SF nanobacteria (Fig. 3G). Control cells were negative (not shown). Standard DNA staining of the nanobacteria-infected cells revealed no ordinary contamination (Fig. 3H). TEM occasionally revealed SF nanobacteria adhering to the cell surface, but mostly they were in various compartments within the cells (Fig. 3 I–L),
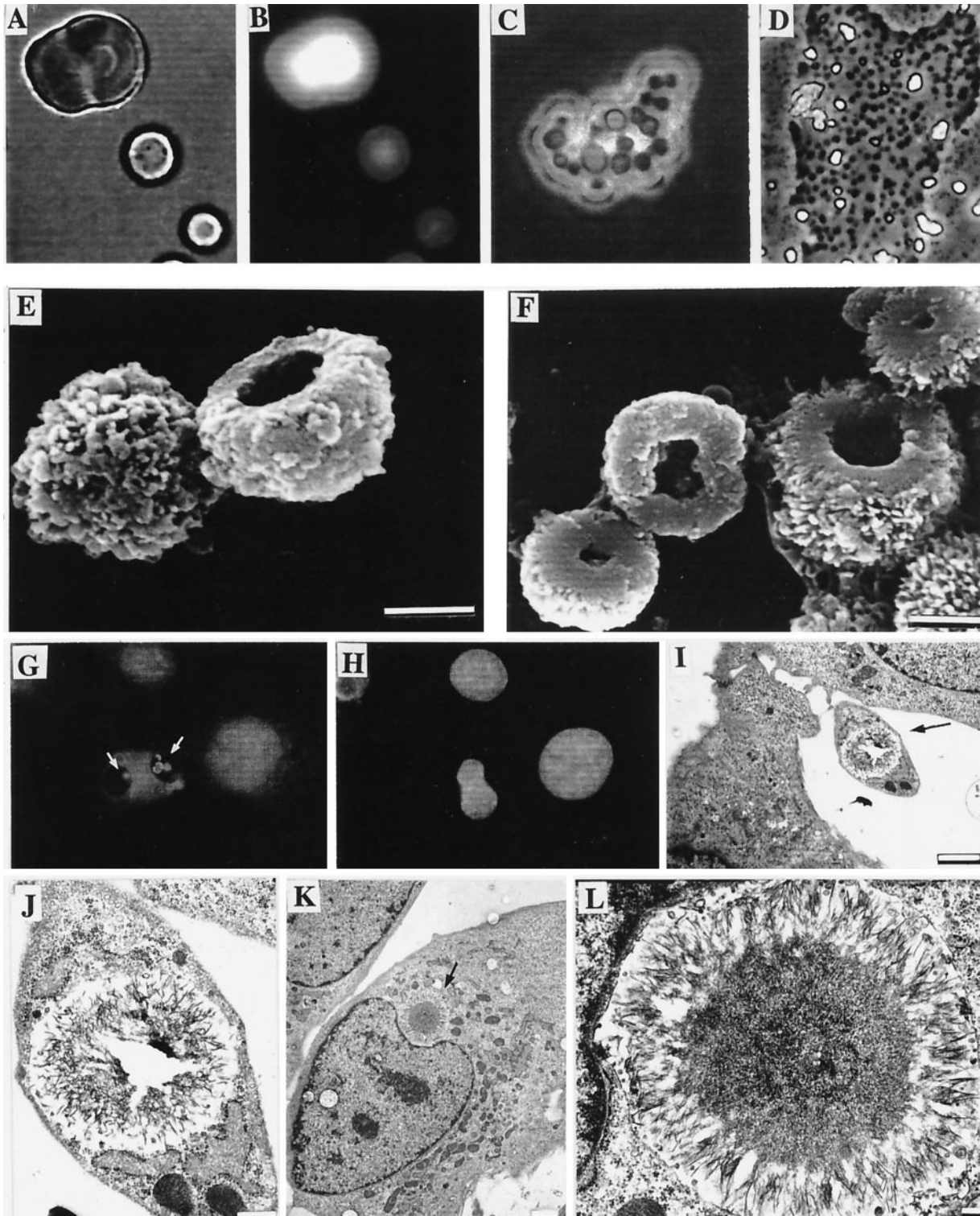

Fig. 3. Nanobacteria cultured under SF conditions and their interaction with cells. (A) Light microscopic micrograph. (B) DNA staining of the same area with the modified Hoechst staining method. (C) DIC images of nanobacteria inside a common apatite shelter. (D) A partly demineralized nanobacterial group (A–D, ×860). (E and F) SEM micrographs of nanobacterial dwellings detached from the culture vessel. (Bars = 1 μm.) (G) IIFS of internalized mineralized nanobacteria (white arrows) in 3T6 cells. (H) DNA staining of the same area with standard Hoechst method. (×540.) (I–L) TEM micrographs of intracellular calcifications in 3T6 cells caused by SF nanobacteria. (Bars: I and K = 2 μm; J = 500 nm; L = 200 nm.)
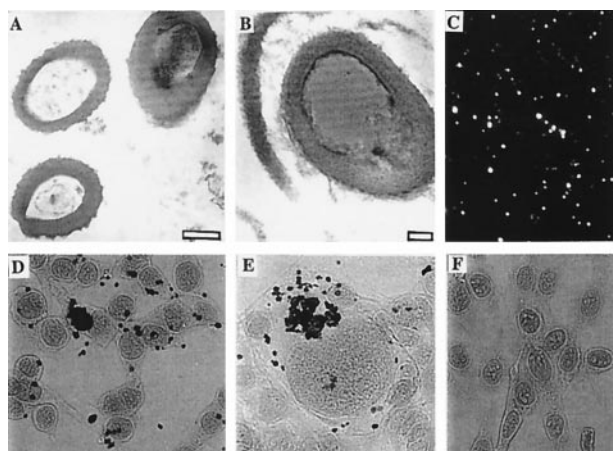
FIG. 4. Examples of extra- and intracellular calcification by nanobacteria. TEM micrograph of cultured nanobacteria (bar = 200 nm) from FBS (*A*) and a bacterium in a kidney stone after demineralization (*B*; bar = 50 nm). (*C*) IIFS of the same kidney stone with anti-nanobacteria mAb. (*D* and *E*) von Kossa staining results of 3T6 cells exposed to SF nanobacteria for 24 hr. (*F*) Negative control. (×270.)

including nucleus (not shown). von Kossa staining revealed intra- and extracellular calcification in these cells (Fig. 4 *D* and *E*). Heavily infected cells showed nuclear abnormalities, e.g., macronucleus, as shown in Fig. 4*E*, and abnormal nuclear shape (Fig. 3 *G, H, K*, and *L*). Control cells were von Kossa negative and did not have nuclear abnormalities (Fig. 4*F*).

Detection of Nanobacterial Antigens in Kidney Stones. We performed a pilot survey on 30 human kidney stones to assess whether nanobacteria can be found. Nanobacteria-specific mAb detecting a protein epitope (5) revealed positive, nanobacteria-sized cocci at various concentrations in all 30 demineralized stones using IIFS. Image of a relevant sample is seen in Fig. 4*C*. The results could be repeated with another nanobacteria-specific mAb, Nb 5/2, that detects a carbohydrate epitope and the binding could be abolished with sodium borohydride treatment, which destroys carbohydrate antigens. Specificity was further proven with negative staining results with four different mAbs (IgG$_1$ class) detecting nonrelevant antigens (data not shown). Bacteria of similar size and morphology (Fig. 4*B*) as nanobacteria (Fig. 4*A*) were found in strongly positive stones using TEM (Fig. 4 *B* and *C*). In nanobacterial culture conditions, sterile-filtered extracts of all of the stones revealed microorganisms having the growth rate, morphology, mineralization, and staining properties of nanobacteria.

DISCUSSION

We have found nanobacterial culture systems that allow for reproducible production of apatite calcification *in vitro*. Depending on culture conditions, tiny nanocolloid-sized particles covered with apatite or biofilm, sand, stones, and tumor-like growths of apatite could be produced (Table 1). The principal precondition for mineralization was low levels of intact serum in the culture medium. Serum contains powerful proteinaceous inhibitors of apatite crystal formation, osteopontin, osteocalcin (1), and fetuin (18), which may account for the observed inhibition and even dissolution of the formed minerals after replenishment of FBS. In cases of nanobacterial cultures in serum-containing medium, the inhibitors permitted only marginal mineralization. Mineralization increased in parallel with the dilution of the serum in cell culture medium. Finally, in SF medium, apatite formation was extensive and rapid. Although modified Loeffler medium contains 75% serum, the serum proteins were denatured during the steril-

Table 1. Culturability of nanobacteria and apatite formation

Culture condition	Replication	Size	Apatite and its form
Serum	+	S	+, nanocolloid
10–50% serum in DMEM	+	S	++, nanocolloid
DMEM	+	L	+++, sand
50% DMEM-50% urine	+	L	+++, sand
Urine	+/−	n.e.	n.e.
Modified Loeffler medium	+	L	+++, tumor-like

S, small size (200–400 nm); L, large size (1 μm to 1 mm, including the mineral). n.e., not evaluated because of crystal formation. Pluses in the last column refer to amount.

ization steps. Thus, apatite formation was not inhibited, resulting in solid apatite colonies about 1–5 mm in diameter in 6 wk. Living nanobacteria are needed to produce apatite in the nanobacterial model. γ-Irradiated nanobacteria did not multiply and, although they could gather apatite on them, no sizable calcification was produced even after 6-mo incubations.

Chemical analysis revealed that the overall composition of biofilm and solid mineral formation was similar to that of bone, except carbonate apatite was formed, as in most extraskeletal tissue calcification and stones, whereas in bone, hydroxyapatite is the prevalent form. Only a few models have been published for studying apatite mineralization *in vitro* (19–21), e.g.,: (*i*) Bacterial models of (kidney) stones using bacteria having urease and often AP activity (22, 23). (*ii*) Osteoblastic cell cultures for studying bone formation. Generally, the apatite formation required elevated P$_i$ and/or Ca^{2+} levels and AP activity (24). (*iii*) Gel and other inorganic crystallization models that usually used saturated or supersaturated solutions of Ca^{2+} and P$_i$ with or without macromolecular components for crystallization (19, 20). In the nanobacterial model, apatite was formed at [Ca] 1.8 mM and [P$_i$] 0.9 mM or less, without replenishment of the medium.

Nanobacteria may induce calcification and stone formation *in vivo* because: (*i*) Nanobacteria have been detected in human blood (10). (*ii*) Nanobacteria have been shown to be transported from blood into urine as living organisms (6). (*iii*) Nanobacterial antigens were found in human kidney stones. (*iv*) Nanobacteria were shown to infect phagocytosing cells (fibroblasts), resulting in intra- and extracellular calcification visible with von Kossa stain and with a similar concentric layer appearance as Michaelis–Gutmann calcospherules found in malacoplakia.

Malacoplakia is a rare chronic inflammatory disease of unknown cause, but a bacterial factor has been implicated. The disease occurs as tumoral growths in urogenital system (bladder, kidney, ureter, and urethra) characterized by an intensive infiltrate of histiocytes containing intra- and extracellular calcospherules composed of apatite. Their size and structure in TEM (25) closely resemble that of our calcified nanobacteria. The possible role of nanobacteria in Michaelis–Gutmann body formation requires further investigation.

Apatite may play a key role in the formation of all kidney stones. The crystalline components of urinary tract stones are calcium oxalate, calcium phosphate, struvite, purines, or cystine. The majority of urinary stones are admixtures of two or more components, with the primary admixture being calcium oxalate and apatite (26). Furthermore, fermentor model studies have shown that calcium phosphate nidi are always formed initially and may subsequently become coated with calcium oxalate or other components (27). SEM reveals the great similarity in size and morphology of SF nanobacteria and human kidney stones (ref. 28; http://www.herringlab.com/sems/sems 2.html) that are formed from small apatite units.

Medical Sciences: Kajander and Çiftçioglu

Proc. Natl. Acad. Sci. USA 95 (1998) 8279

Nanobacteria were found in all 30 human kidney stones that we have screened. In animal experiments, radiolabeled nanobacteria were efficiently excreted from the blood into urine (6). Previously, only struvite stones (4–15% of all kidney stones) composed of magnesium ammonium phosphate and small amounts of apatite have been regarded as deriving from bacteria. They are formed *in vitro* and probably *in vivo* by *Proteus*, staphylococci, and *Escherichia coli* that produce urease (29), elevating the local pH to more lithogenic levels. AP may augment the lithogenicity. Nanobacteria do not produce urease or AP, but nucleate carbonate apatite directly on their surfaces at pH 7.4, suggesting the presence of nucleating molecules. Since nanobacteria are culturable under physiological conditions in media similar in composition to glomerular filtrate, nanobacteria offer a unique model for kidney stone formation.

Tissue calcification of carbonate apatite in nature is common in other diseases, e.g., atherosclerotic plaques accumulate calcium phosphate. Hemodialysis patients can develop extensive metastatic and tumoral calcification with mechanisms not totally understood (30). Acute periarthritis is apatite arthropathy related to intratendinous calcifications. Apatite crystals are also known to cause inflammation when injected into the synovial space (31). Tissue calcification is found in several malignant diseases (25). Many malignant cells have receptors for nanobacterial adherence (5) that could introduce nanobacteria into the tumor with subsequent calcification, as shown here with von Kossa staining of transformed fibroblasts.

Human and bovine nanobacteria grow similarly, share the same surface antigens and other special features, and both produce carbonate apatite. The possible role of nanobacteria in a variety of pathological calcification conditions is under investigation. In the interim, nanobacteria represent a unique model for evaluating calcification *in vitro* under physiological conditions.

1. Robey, P. G. & Boskey, A. L. (1996) in *Osteoporosis*, eds. Marcus, R., Feldman, D. & Kelsey, J. (Academic, San Diego), pp. 95–183.
2. Folk, R. L. (1993) *J. Sediment. Petrol.* **63,** 990–999.
3. Sillitoe, R. H., Folk, R. L. & Saric, N. (1996) *Science (Washington DC)* **272,** 1153–1155.
4. Mojzsis, S. J., Arrhenius, G., McKeegan, K. D., Harrison, T. M., Nutman, A. P. & Friend, C. R. L. (1996) *Nature (London)* **384,** 55–59.
5. Çiftçioglu, N. & Kajander, E. O. (1998) *Pathophysiology* **4,** 259–270.
6. Åkerman, K. K., Kuikka, J. T., Çiftçioglu, N., Parkkinen, J., Bergström, K. A., Kuronen, I. & Kajander, E. O. (1997) *SPIE Proc.* **3111,** 436–442.
7. Kajander, E. O., Kuronen, I., Åkerman, K., Pelttari, A. & Çiftçioglu, N. (1997) *SPIE Proc.* **3111,** 420–428.
8. Åkerman, K., Kuronen, I. & Kajander, E. O. (1993) *Scanning* **15,** 90–91.
9. Kajander, E. O., Tahvanainen, E., Kuronen, I. & Çiftçioglu, N. (1994) *Zentralbl. Bakteriol. Suppl.* **26,** 147–149.
10. Çiftçioglu, N., Kuronen, I., Åkerman, K., Hiltunen, E., Laukkanen, J. & Kajander. E. O. (1997) in *Vaccines 97*, eds. Brown, F., Burton, D., Doherty, P., Mekalanos, J. & Norrby, E. (Cold Spring Harbor Lab. Press, Cold Spring Harbor, NY), pp. 99–103.
11. Nash, P. & Krenz, M. M. (1991) in *Manual of Clinical Microbiology*, eds. Balows, A., Hausler, W. J., Jr., Herrmann, K. L., Isenberg, H. D. & Shadomy, H. J. (American Society for Microbiology, Washington, DC), p. 1257.
12. Luna, L. G. (1968) in *Manual of Histologic Staining Methods of the Armed Forces Institute of Pathology*, ed. Luna, L. G. (McGraw–Hill, New York), pp. 174–188.
13. Suzuki, T., Yano, M., Sumi, S., Honda, M., Hosoya, Y. & Yoshida, K. I. (1997) *Urol. Int.* **58,** 88–92.
14. Blijenberg, B. G., van Vliet, M. & Zwang, L. (1997) *Eur. J. Clin. Chem. Clin. Biochem.* **35,** 625–630.
15. Hyvönen, P. M., Hanhijärvi, H. & Ahosilta, K. (1986) *Acta Pharmacol. Toxicol.* **59,** 129–134.
16. Koneman, E. W., Allen, S. D., Janda, W. M., Schreckenberger, P. C. & Winn, C. W., Jr. (1992) in *Color Atlas and Textbook of Diagnostic Microbiology* (Lippincott, Philadelphia), p. 178.
17. Çiftçioglu, N., Pelttari, A. & Kajander, E. O. (1997) *SPIE Proc.* **3111,** 429–435.
18. Schinke, T., Amendt, C., Trindl, A., Poschke, O., Muller-Esterl, W. & Janhen-Dechent, W. (1996) *J. Biol. Chem.* **271,** 20789–2096.
19. Achilles, W., Jöckel, U., Schaper, A., Burk, M. & Riedmiller, H. (1995) *Scanning Micros.* **9,** 577–586.
20. Boskey, A. L. (1989) *J. Phys. Chem.* **93,** 1628–1633.
21. Stanford, C. M., Jacobson, P. A., Eanes, E. D., Lembke, L. A. & Midura, R. J. (1995) *J. Biol. Chem.* **270,** 9420–9428.
22. McLean, R. J., Nickel, J. C., Noakes, V. C. & Costerton, J. W. (1985) *Infect. Immun.* **49,** 805–811.
23. McLean, R. J., Nickel, J. C., Beveridge, T. J. & Costerton, J. W. (1989) *J. Med. Microbiol.* **29,** 1–7.
24. Stanford, C. M., Jacobson, P. A., Eanes, E. D., Lembke, L. A. & Midura, R. J. (1995) *J. Biol. Chem.* **270,** 9420–9428.
25. Ho, K. L. (1989) *Arch. Pathol. Lab. Med.* **113,** 874–879.
26. Mandel, N. (1996) *Semin. Nephrol.* **16,** 364–374.
27. Leusmann, D. B. & Sabinski, F. (1996) *Urol. Res.* **24,** 73–78.
28. Kajander, E. O., Björklund, M. & Çiftçioglu, N. (1998) in *Enigmatic Microorganisms and Life in Extreme Environments* ed. Seckcbach, J. (Kluwer, The Netherlands), in press.
29. Hugosson, J., Grenabo, L., Hedelin, H., Petterson, S. & Seeberg, S. (1990) *J. Urol.* **143,** 965–968.
30. Zins, B., Zingraff, J., Basile, C., Petitclerc, T., Urena, P., Bardin, T. & Drueke, T. (1992) *Nephron* **60,** 260–267.
31. Hamada, J. (1995) *Nippon Seikeigeka Gakkai Zasshi* **69,** 1158–1169.